J Solid State Electrochem (2010) 14:1629–1635
DOI 10.1007/s10008-010-1004-1

ORIGINAL PAPER

Preparation of Fe_2O_3-exfoliated graphite composite and its electrochemical properties investigated in alkaline solution

Jan Urbaniak · Jan M. Skowroński · Barbara Olejnik

Received: 23 July 2009 / Revised: 22 December 2009 / Accepted: 4 January 2010 / Published online: 2 February 2010

Abstract In the present work, a simple method of preparation of $FeCl_4^-$- graphite intercalation compounds from $HCl/FeCl_3$ solution with the aid of chemical oxidant is presented. Based on X-ray diffraction measurements it was concluded, that stages 8, 6, and 5 $FeCl_4^-$-graphite intercalation compounds were obtained. The compounds thus obtained were thermally treated to obtain Fe_2O_3-exfoliated graphite composites. The dispersion of Fe_2O_3 in the exfoliated graphite flakes was examined with the aid of the energy dispersive X-ray analysis combined with a scanning electron microscopy. Electrochemical behavior of electrodes was investigated in 6 M KOH solution. Electrochemical investigations proved the formation of FeOOH on the surface of exfoliated graphite during the anodic process. Besides, electrochemical investigations showed that the lower limit potential strongly affects the redox behavior of the Fe_2O_3-EG electrode.

Keywords Graphite intercalation compound · Exfoliated graphite · Fe_2O_3 · Exfoliated graphite-iron oxide composite · Cyclic voltammetry

Electronic supplementary material The online version of this article (doi:10.1007/s10008-010-1004-1) contains supplementary material, which is available to authorized users.

J. Urbaniak · J. M. Skowroński (✉)
Institute of Chemistry and Technical Electrochemistry,
Poznan University of Technology,
ul. Piotrowo 3,
60-965 Poznan, Poland
e-mail: jan.skowronski@put.poznan.pl

B. Olejnik
Institute of Non-Ferrous Metals, Branch in Poznan,
Central Laboratory of Batteries and Cells,
Forteczna 12,
61-362 Poznan, Poland

Introduction

Precious metals and metal oxide catalysts are used for many important synthesis reactions in chemical industry. Special interest is paid to supported catalysts, which allow a high dispersion and stabilization of small metallic particles. Among supports, carbons such as activated carbon, carbon black, graphite, and graphitized material are used [1]. The usage of carbon as a support has many advantages. Carbons have a good stability in both acidic and basic media. Besides, after usage, carbon can be burnt off, for it does not produce large amounts of solid waste that need to be landfilled.

Studies on the usage of an iron/carbon composite as anode in Fe-air battery showed that the use of Fe/C composites instead of Fe electrode has some advantages [2]. In the Fe-air batteries, the utilization of iron particles is limited only to a surface thin layer of iron particles. When very small particles of iron are used instead larger particles, the capacity of iron electrode increases, however, it deteriorates rapidly during the discharge/charge cycles [3]. If Fe/C composites are used instead pure iron, the Fe/C electrode shows both improved conductivity and charge-discharge performance. In order to increase the active material surface area, Fe_2O_3-loaded carbon composite electrodes are prepared [4-6]. Fe_2O_3-loaded carbon composite electrodes were obtained using various carbon materials such as vapor-grown carbon fibers, acetylene black, natural graphite and carbon nanofibers of the nanotube type. It was found that the type of carbon plays an important role in determining the electrochemical properties of Fe_2O_3-loaded carbon electrodes [4-6].

The use of exfoliated graphite as a catalyst support was reported in ref. [7]. One of the peculiarities of exfoliated graphite (EG) is its low bulk density [8-11]. Exfoliated

graphite is commonly produced via thermal treatment of graphite intercalation compounds (GIC). Graphite intercalation compounds are prepared through insertion of chemical species (atoms, ions, molecules) into interlayer spacings of graphite [12]. The guest chemical species and the process of insertion are called intercalate and intercalation, respectively. In general, intercalation methods can roughly be classified into two groups: chemical and electrochemical ones.

Intercalation of $FeCl_3$ into graphite resulting in the formation of $FeCl_3$-GIC may be carried out both chemically, by a vapor-phase [13, 14] or a liquid-phase reaction [15-17], and electrochemically [17, 18]. During intercalation from a liquid phase, molecules of solvent are intercalated together with intercalate, giving GICs with properties different from those of the corresponding binary GIC consisting of graphite and intercalate. These molecules can influence the process of exfoliation to bring about more expanded material due to vaporization of solvent.

In this study, a simple method of preparation of $FeCl_4^-$-GICs from $HCl/FeCl_3$ solution with the aid of chemical oxidant is presented. $FeCl_4^-$-GICs thus obtained were thermally treated to obtain Fe_2O_3-exfoliated graphite composites of which electrochemical properties were investigated in alkaline solution.

Experimental

Syntheses of GICs were performed from concentrated hydrochloric acid. Natural graphite (Graphitwerk Kropfmühl AG, Germany, average flake size: 180–200 μm) was immersed into 12 M aqueous solution of HCl. The molar ratio of graphite to CrO_3 was chosen to be 1:0.25, whereas the molar ratio of graphite to $FeCl_3$ was equal 1:2. The mixture of graphite/CrO_3/$FeCl_3$/HCl was put into flask and kept at room temperature for three different periods of time: 5, 15 and 25 hours. The reaction products were filtered and washed out with a large amount of 6 M HCl solution to remove any adhering iron chloride, followed by acetone and then stored in moisture free atmosphere. For characterizing the structure of GIC, the X-ray diffraction (XRD) measurements were performed using CuK_α radiation. The preparation of Fe_2O_3-EG composites for the XRD measurements included the formation of very thin layer of the investigated sample by pressing into a profile-milled plate. Similar procedure was used in our previous papers [11, 19, 20]. For observing the concentration profiles of intercalates in GIC and EG the energy dispersive X-ray (EDX) analysis combined with a scanning electron microscopy (SEM) was used. To obtain exfoliated graphite, GICs were put into open ceramic boats and then were thermally treated at 800 °C in air atmosphere. After exfoliation, each EG was put in the same manner into calibrated cylinder, the bulk volume per unit weight of exfoliated graphite flakes was measured and then the bulk density of each sample was calculated.

Electrochemical behavior of EG electrodes was investigated in a three-electrode system with a potentiostat-galvanostat PGSTAT30 Autolab (EcoChemie B.V.). The Hg/HgO/6 M KOH system (E=0.098 V vs. standard hydrogen electrode) was employed as the reference electrode. All potentials throughout the paper are referred to this electrode. Platinum wire was used as a counter electrode. The electrolyte was 6 M KOH solution. The cyclic voltammetric (CV) measurements were carried out in three potential ranges: −1.05↔0.1 V, −1.15↔0.1 V and −1.25↔0.1 V. Starting from the rest potential of electrode with a scan rate 5 mV/s, the potential was changed in the negative direction (cathodic polarization). After the reversal of polarization direction the potential was changed in the positive direction (anodic polarization). All electrochemical measurements were carried out at room temperature.

Results and discussion

When anhydrous $FeCl_3$ is placed into concentrated hydrochloric acid, the most important complex formed in such a medium is $FeCl_4^-$ anion [21]. So far, intercalation of $FeCl_3$ into graphite from HCl solutions resulting in the formation of $FeCl_4^-$-GIC was successfully made by electrochemical oxidation [18]. Opposite to this, Fig. 1 presents XRD pattern of compound prepared with the aid of chemical oxidant. GIC was obtained after 5 h immersion of natural graphite in $FeCl_3$/HCl solution with a small addition of CrO_3. As seen from XRD pattern, the reaction resulted in stage-8 $FeCl_4^-$-GIC (I_c=3.28 nm) admixed with the phase of unreacted graphite. The EDX profiles for Fe and Cl (Fig. 2) confirmed the existence of intercalate ($FeCl_3$) between graphene layers. As can be seen from this Figure,

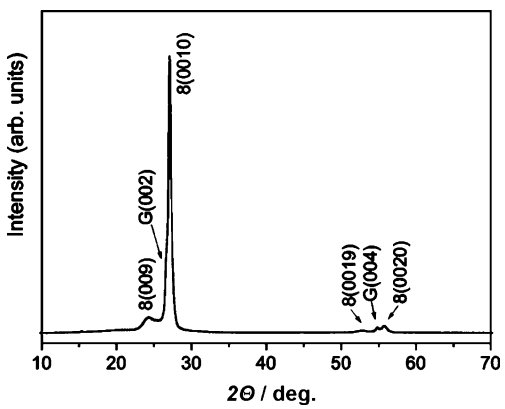

Fig. 1 X-ray pattern of stage-8 $FeCl_4^-$-GIC admixed with the phase of unreacted graphite (G)

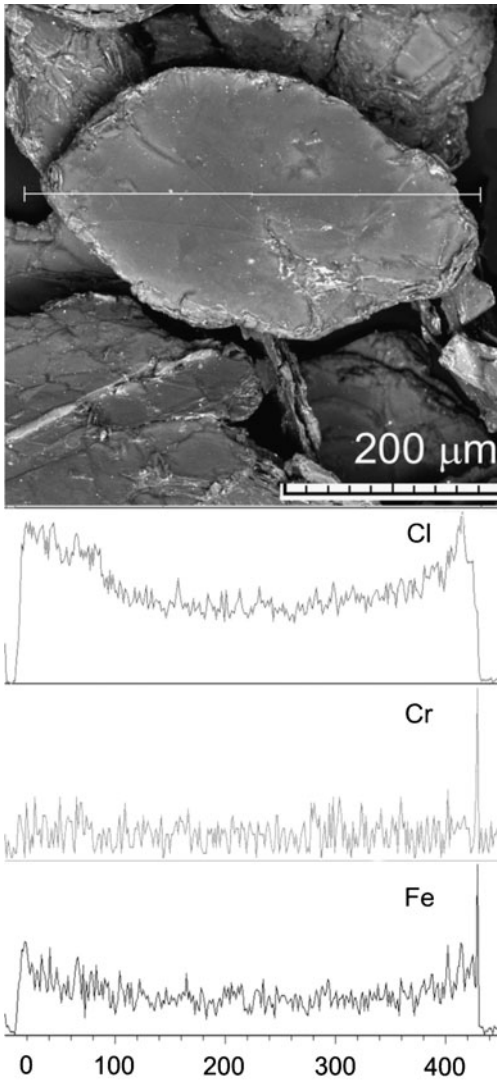

Fig. 2 SEM micrograph and EDX distribution curves for Cl, Cr, and Fe of the flake $FeCl_4^-$-GIC

the distribution of intercalate is not uniform. The intensities of iron and chlorine profiles are the highest near the flake edges, whereas the intensity lines are descending towards the flake center. Despite the presence of CrO_3 in the reaction solution, the distribution line of Cr examined for stage-8 $FeCl_4^-$-GIC is quite flat and its intensity does not surpass the base line. This feature suggests that no CrO_3 was intercalated into graphite.

Figure 3 presents XRD pattern for GIC obtained after the time of synthesis prolonged to 15 hours. From this pattern it was calculated that the product of synthesis was built up of domains of stage-6 $FeCl_4^-$-GIC (I_c=2.62 nm, d_i=0.94 nm) admixed with the phase of unreacted graphite (peaks G (002) and G(004)).

Figure 4 presents XRD pattern for GIC obtained after the time of synthesis prolonged to 25 h. As seen from this pattern, the product of synthesis was stage-5 $FeCl_4^-$-GIC

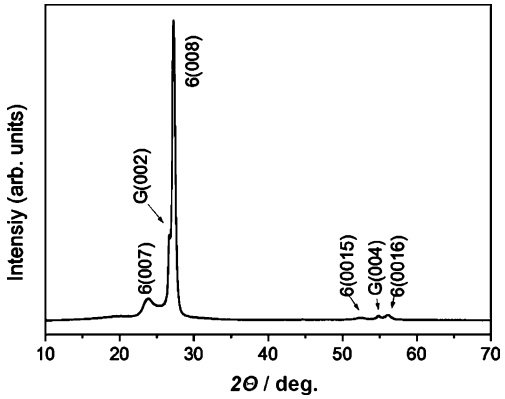

Fig. 3 X-ray pattern of stage-6 $FeCl_4^-$-GIC admixed with the phase of unreacted graphite (G)

(I_c=2.28 nm, d_i=0.94 nm). The phase of unreacted graphite was also present. The distribution profiles for intercalates bonded between graphene layers are presented in Figure 5. A comparison for the EDX profiles for Fe and Cl shows that the intensities of iron and chlorine across the graphite flake are closed to each other. These results allows the conclusion that no intercalation of CrO_3 took place and the role of CrO_3 in the reaction mixture during the process of intercalation of $FeCl_4^-$ into natural graphite conducted from the solution of $FeCl_3/CrO_3$ in concentrated HCl is limited to the oxidation of the host graphite.

When GICs are heat treated at high temperature the process of exfoliation of host graphite takes place resulting in the formation of exfoliated graphite (EG) During the process of exfoliation of $FeCl_3$-GIC carried out in an inert atmosphere $FeCl_3$ is partially removed from the interlayer spaces of the graphite flake and the remainder is reduced to $FeCl_2$ [22]. If the process of exfoliation is carried out in air atmosphere, except deintercalation, the conversion of $FeCl_4^-$ into iron oxides should be taken into consideration. Table 1 presents bulk densities obtained after exfoliation of

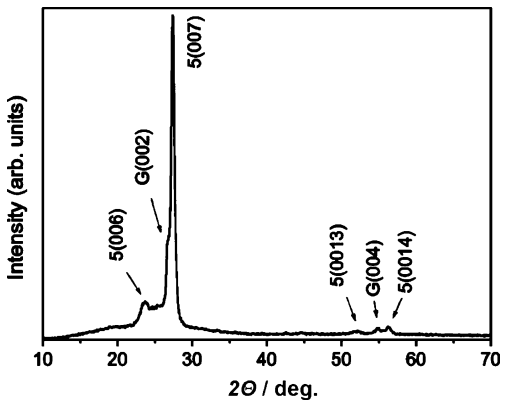

Fig. 4 X-ray pattern of stage-5 $FeCl_4^-$-GIC admixed with the phase of unreacted graphite (G)

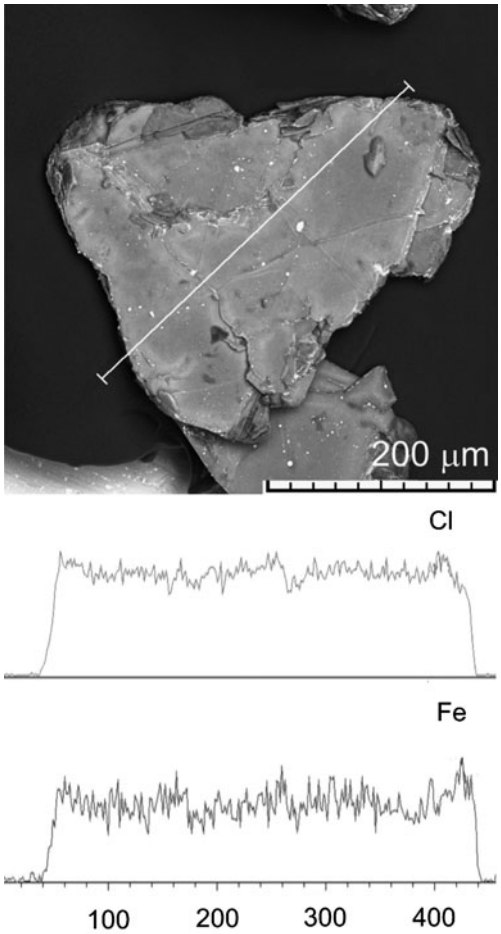

Fig. 5 SEM micrograph and EDX distribution curves for Cl, and Fe of the flake $FeCl_4^-$-GIC

synthesized $FeCl_4^-$-GICs. The smallest bulk density of stage-5 $FeCl_4^-$ -GIC means that its exfoliation degree is the largest. Two sets of SEM micrographs combined with the EDX profiles for Fe, Cl and O obtained for exfoliated stage-5 $FeCl_4^-$-GIC are presented in Fig. 6. As revealed by SEM analysis, exfoliated $FeCl_4^-$-GIC exhibits a worm-like structure. Small bright spots are observed on the graphite surface. Higher amount of these spots is located near the edges of exfoliated particles. Taking into account that the process of exfoliation of $FeCl_4^-$-GIC was carried out on contact with oxygen of air atmosphere, it is likely that the spots are related to the presence of iron oxides. As can be

Table 1 Bulk densities obtained after exfoliation of $FeCl_4^-$-GICs

$FeCl_4^-$-GIC	Bulk density after exfoliation (cm^3)
Stage-8	0.019
Stage-6	0.016
Stage-5	0.011

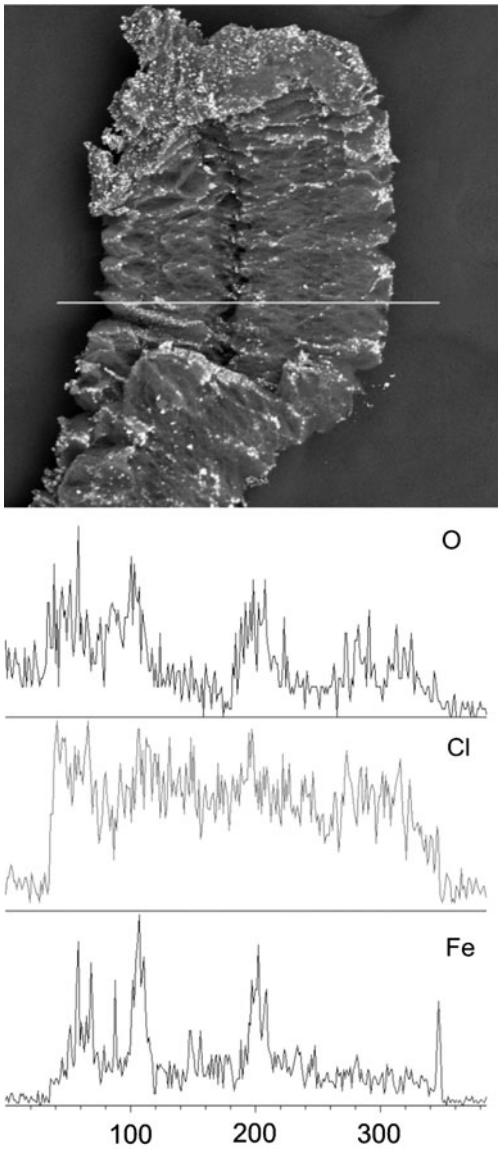

Fig. 6 SEM micrograph and EDX distribution curves for O, Cl, and Fe obtained for exfoliated stage-5 $FeCl_4^-$-GIC

seen from the EDX profiles, the intensity of the chlorine signal is very high and uniform as measured across the particle of exfoliated compounds. Contrary to this, the lines for iron and oxygen contain many deep leaps. Moreover, the profiles corresponding to the arrangement of Fe and O displays a high coincidence which corroborates the existence of iron oxides formed due to exfoliation. The composition of the obtained material was analyzed by the energy dispersive X-ray analysis. For analysis, ten randomly chosen areas (50 μm^2 each) were investigated. The EDX semi-quantitative analysis gave the atomic ratios of Fe/O and Fe/Cl to be 1:3.2 and 1:0.4, respectively. An average Fe content in the composite was equal to ca. 7 wt.%.

In Fig. 7, XRD pattern obtained for exfoliated stage-5 $FeCl_4^-$-GIC is shown. The diffraction peaks related to the

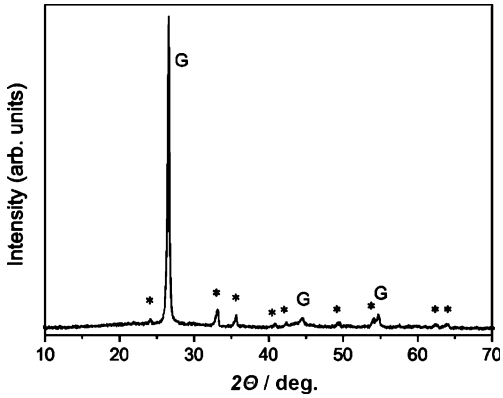

Fig. 7 XRD pattern obtained for exfoliated stage-5 $FeCl_4^-$-GIC: α-Fe_2O_3 phase (*asterisk*), graphite phase (G)

graphite phase (marked with G letter) together with *hkl* reflections characteristic of the α-Fe_2O_3 phase are observed. A comparison of the experimental interplanar spacings calculated based on the pattern of Fig. 7 with the theoretical values for α-Fe_2O_3 phase is gathered in Table 2. It is very likely, that during the formation of Fe_2O_3 at the graphite-iron oxide interphase a thin layer of FeO phase forms due to the reduction reaction of Fe_2O_3 by graphite carbon.

The cyclic voltammograms recorded for electrodes made of Fe_2O_3-EG, obtained due to exfoliation of stage-5 $FeCl_4^-$-GIC, are shown in Figs. 8, 9, and 10. Figure 8 presents CV curves recorded for electrode Fe_2O_3-EG, which was cycled in the potential range −1.15↔0.1 V. Starting from the rest potential of the electrode (0.04 V) towards negative direction, a huge irreversible cathodic peak with the current maximum at −0.72 V is recorded. The origin of this peak, appearing only in the first negative run starting from the rest potential of the electrode, is not yet clear. One of the possible explanation may be the reduction of some functional groups (oxygen or/and chlorine) generated on the surface of porous exfoliated graphite during the process of exfoliation. The oxygen excess in relation to iron atoms in the formed Fe_2O_3, estimated by the EDX analysis, supports this assumption. On the other hand, it cannot be excluded that the cathodic reduction of Fe_2O_3 in strongly alkaline solution, resulting in the formation of $HFeO_2^-$ ions according to eq. 1, contributes to this peak area in parallel.

$$Fe_2O_3 + H_2O + 2e^- \rightleftarrows 2HFeO_2^- \quad (1)$$

After the reversal of polarization, a small anodic current peak at −0.77 V precedes a double peak with the current maxima at −0.56 and −0.47 V. The CV curves for successive cycles differ from the first one. On further cycling, a sharp cathodic peak with the current maximum at −0.98 V (C_1) and the corresponding anodic peak at −0.59 V (A_1), with a preceding shoulder at around −0.74 V, are observed. The cathodic peak C_1 may be attributed to the reduction of Fe(III) to $Fe(OH)_2$, whereas the anodic peak A_1 corresponds to the oxidation of $Fe(OH)_2$ to Fe(III) [23]. The anodic oxidation of $Fe(OH)_2$ may involve two reactions [23]:

$$Fe(OH)_2 + OH^- \rightleftarrows FeOOH + H_2O + e^- \quad (2)$$

and/or [24]

$$3Fe(OH)_2 + 2OH^- \rightleftarrows Fe_3O_4 + 4H_2O + 2e^- \quad (3)$$

On the repetition of cycles, the redox Fe(II)/Fe(III) charge of the (A_1) and (C_1) peak couple gradually increases. When the reduction of $Fe(OH)_2$ continues the

Table 2 A comparison of the experimental interplanar spacings with the theoretical values for α-Fe_2O_3 phase

Reflection number	$d_{measured}$ (nm)	Graphite	α-Fe_2O_3 (JCPDS 33-0664)		
			$d_{calculated}$ (nm)	*I [%]*	hkl
1	0.368		0.368	30	102
2	0.335	G	–	–	–
3	0.270		0.270	100	104
4	0.252		0.252	70	110
5	0.221		0.221	20	113
6	0.213	G	–	–	–
7	0.204	G	–	–	–
8	0.184		0.184	40	204
9	0.170		0.169	45	116
10	0.168	G	–	–	–
11	0.149		0.148	30	214
12	0.145		0.145	30	300

G graphite reflections observed in Fig. 7

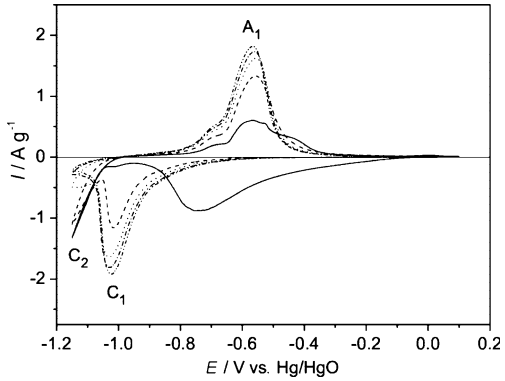

Fig. 8 CV curves recorded for electrodes made of Fe_2O_3-EG, obtained due to exfoliation of stage-5 $FeCl_4^-$-GIC: cycle 1 (——), cycle 2 (- - -), cycle 3 (· · ·), cycle 4 (- · -), cycle 5 (- ·· -). Potential range: −1.15 V↔0.1 V

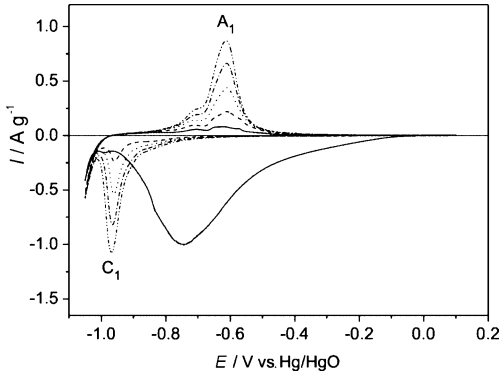

Fig. 10 CV curves recorded for electrodes made of Fe_2O_3-EG, obtained due to exfoliation of stage-5 $FeCl_4^-$-GIC: cycle 1 (——), cycle 2 (- - -), cycle 3 (· · ·), cycle 4 (- · -), cycle 5 (-··-). Potential range: −1.05 V↔0.1 V

formation of Fe takes place. According to the authors of ref. [25] it involves the following partial steps:

$$Fe(OH)_2 + e^- \rightleftarrows [Fe(OH)]_{ad} + OH^- \quad (4)$$

$$[Fe(OH)]_{ad} + e^- \rightleftarrows Fe + OH^- \quad (5)$$

Moreover, the formation of $Fe(OH)_2$ might proceed through the formation of soluble intermediate product, $HFeO_2^-$ [23]:

$$[Fe(OH)]_{ad} + 2OH^- \rightleftarrows HFeO_2^- + H_2O + e^- \quad (6)$$

and

$$HFeO_2^- + H_2O \rightleftarrows Fe(OH)_2 + OH^- \quad (7)$$

As can be seen in Fig. 8, the Fe(II)/Fe redox couple is not observed. The similar lack of the Fe(II)/Fe redox couple was reported by Hang et al. [4] who investigated the behavior of Fe_2O_3-loaded carbon electrodes. The lack of the Fe(II)/Fe redox couple during electrochemical measurements, they ascribed to the insulating nature of the $Fe(OH)_2$ active material, which could inhibit the Fe/Fe(II) redox couple, causing a large overpotential.

In order to observe the presence of the Fe/Fe(II) redox couple, the CV measurements were carried out with a lower reversal potential of −1.25 V (Fig. 9). Starting from the rest potential of electrode (0.05 V) towards negative direction, besides aforementioned huge irreversible cathodic peak attributed to the reduction of functional groups on the carbon surface and/or the process of Fe_2O_3 reduction, another cathodic peak (C_2) with the current maximum at −1.2 V is observed. This peak is probably related to the reduction of Fe(III) into Fe(II) according to eq. 2. After the reversal of polarization, a small anodic current peak appears at −0.69 V followed by two anodic peaks with the current maxima at −0.54 and −0.42 V. In the second cycle, a sharp cathodic current peak with the current maximum at −1.03 V (C_1) associated with the reduction of FeOOH to $Fe(OH)_2$, and the corresponding oxidation peak at −0.55 V (A_1) are observed. Contrary to the results obtained within the shorter potential range (Fig. 8), when the CV measurements are carried out with a reversal potential of −1.25 V (Fig. 9), the Fe(II)/Fe(III) redox couple peaks decrease with increasing cycle number. This feature may be due to a gradual growth of a passive layer at the EG particle surface and/or depletion of electrode resulting from dissolving oxide species in the electrolyte. For the third and the following cycles, a tiny anodic peak (A_2), with the current maximum at −0.96 V, may be noticed. This peak is probably due to the oxidation of Fe, thereby confirming that the process of $Fe(OH)_2$ reduction occurred during the cycling. The reason for the invisible cathodic peak corresponding to the reduction of $Fe(OH)_2$ to Fe is probably the overlapping of the cathodic current arising from the reduction reaction of $Fe(OH)_2$ and the hydrogen evolution reaction which occur simultaneously [2].

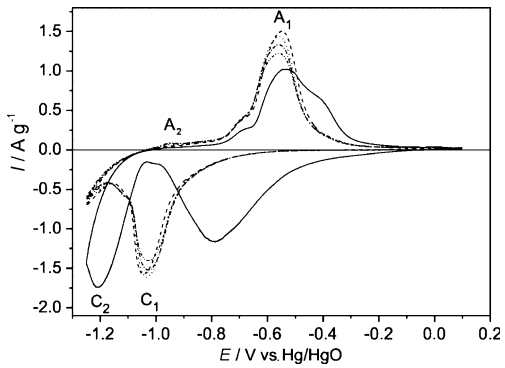

Fig. 9 CV curves recorded for electrodes made of Fe_2O_3-EG, obtained due to exfoliation of stage-5 $FeCl_4^-$-GIC: cycle 1 (——), cycle 2 (- - -), cycle 3 (· · ·), cycle 4 (- · -), cycle 5 (-··-). Potential range: −1.25 V↔0.1 V

Additional information about the electrochemical behavior of the composite Fe_2O_3-EG electrode was obtained during cyclic measurements performed in the shorter potential range: −1.05↔0.1 V (Fig. 10). The CV curves presented in Fig. 10 show that the lower limit potential strongly effect on the redox behavior of the Fe_2O_3-EG electrode. When measurements were carried out with a reversal potential of −1.05 V only a small part of FeOOH is reduced into $Fe(OH)_2$ thereby only a slight anodic response (A_1) is observed after changing the polarization direction. However, on cycling the gradually growing cathodic current peak (C_1) at −0.97 V, attributed to the formation of Fe(II)/Fe(III) redox couple, and the corresponding oxidation peak (A_1) at −0.59 V are observed.

Conclusions

It has been shown a simple chemical method of intercalation of $FeCl_3$ into natural graphite performed from the solution $FeCl_3$/HCl with the aid of admixed CrO_3. Based on XRD measurements supported by EDX analysis, one can conclude that the role of CrO_3 in the solution is limited to the oxidation of the host graphite. Our results demonstrated that exfoliated graphite with highly dispersed Fe_2O_3 phase was obtained due to exfoliation of $FeCl_4^-$-GIC. The dispersion of Fe_2O_3 in the exfoliated graphite flakes is not uniform. The amount of Fe_2O_3 phase is higher near the edges of exfoliated particles. Electrochemical investigations proved the formation of FeOOH on the surface of exfoliated graphite during the anodic process. The results showed that the lower limit potential strongly affects the redox behavior of the Fe_2O_3-EG electrode. The highest activity of the electrode upon the charge/discharge process of Fe(II)/Fe(III) redox couple was found in the potential range −1.15↔0.1 V. On cycling, the electrode in this potential range, the increase of current peaks related to the Fe(II)/Fe(III) redox couple was observed. When the value of the lower limit potential is moved down to −1.25 V the passivation of an electrode is observed as a fast decrease of the charge/discharge capacity of Fe(II)/Fe(III) redox couple on cycling.

References

1. Auer E, Freund A, Pietsch J, Tackle T (1998) Appl Catal A 173:259
2. Hang BT, Eashira M, Watanabe I, Okada S, Yamaki J, Yoon S, Mochida I (2005) J Power Sources 143:256
3. Huang K, Chou K (2007) Electrochem Commun 9:1907
4. Hang BT, Watanabe T, Eashira M, Okada S, Yamaki J, Hata S, Yoon S, Mochida I (2005) J Power Sources 150:261
5. Hang BT, Yoon S, Okada S, Yamaki J (2005) J Power Sources 168:522
6. Hang BT, Hayashi H, Yoon S, Okada S, Yamaki J (2008) J Power Sources 178:393
7. Kuznetsov BN, Chesnokov NV, Mikova NM, Zaikovskii VI, Drozdov VA, Savos'kin MV, Yaroshenko AM, Lyubchik SB (2003) React Kinet Catal Lett 80:345
8. Chung DDL (1987) J Mater Sci 22:4190
9. Skowroński JM (1988) J Mater Sci 23:2243
10. Skowroński JM, Krawczyk P (2004) J Solid State Electrochem 8:442
11. Skowroński JM, Krawczyk P, Rozmanowski T, Urbaniak J (2008) Energy Convers Manage 49:2440
12. Skowroński JM (1997) In: Nalwa HS (ed) Handbook of organic conductive molecules and polymers, Ch. 12. Wiley, Chichester
13. Su SR, Oblas DW (1987) Carbon 25:391
14. Mazurek H, Ghavamishashidi G, Dresselhaus G, Dresselhaus MS (1982) Carbon 20:415
15. Hooley JG (1972) Carbon 10:155
16. Tanaike O, Hoshino Y, Inagaki M (1999) Synth Met 99:105
17. Kang F, Leng Y, Zhang T-Y, Li B (1998) Carbon 36:383
18. Shioyama H, Crespin M, Seron A, Setton R, Bonnin D, Beguin F (1993) Carbon 31:223
19. Skowroński JM, Walkowiak M (2003) J Solid State Electrochem 8:23
20. Skowroński JM, Błażewicz S, Walkowiak M (2006) J New Mater Electrochem Syst 9:353
21. Luter MD, Wertz DL (1981) J Phys Chem 85:3542
22. Begin D, Alain E, Furdin G, Mareche JF (1996) J Phys Chem Solids 57:849
23. Chakkaravarthy C, Perasamy P, Jegannathan S, Vasu KI (1991) J Power Sources 35:21
24. Vijayamohanan K, Shukla AK, Sathyanarayana S (1990) J Electroanal Chem 295:59
25. Cerny J, Micka K (1989) J Power Sources 25:111